第 30 卷第 7 期
2013 年 7 月

控 制 理 论 与 应 用
Control Theory & Applications

Vol. 30 No. 7
Jul. 2013

DOI: 10.7641/CTA.2013.12121

干扰下的无人直升机自适应反步法鲁棒跟踪控制

贺跃帮[1], 裴海龙[1†], 周洪波[2], 孙太任[3]

(1. 华南理工大学 自主系统与网络控制教育部重点实验室, 广东 广州 510640;

2. 湖南理工学院 机械工程学院, 湖南 岳阳 414006; 3. 江苏大学 电气信息工程学院, 江苏 镇江 212013)

摘要: 针对无人直升机干扰下的鲁棒轨迹跟踪问题, 设计了一种自适应反步控制方法. 鉴于作用在直升机上的干扰是产生跟踪误差的主要原因, 该方法的主要思想是寻求一种方法来补偿这种干扰. 首先, 将未建模动态如外部阵风干扰、配平误差、机身、垂尾、平尾以及其他可忽略的动态产生的力和力矩看成一种组合干扰, 从而建立了一个方便反步法控制器设计的简化模型. 当设计好反步法控制器后, 设计了一个非线性自适应律来估计这种组合干扰, 并通过将干扰估计值整合到反步控制器中, 使得闭环跟踪系统的鲁棒稳定性得到了保证, 即基于李雅普诺夫稳定性理论证明了所设的控制器对于干扰主动阻隔, 特别是低频干扰的主动阻隔是有效的. 最后, 两个仿真研究验证了该方法是优于常规反步法和积分反步法的.

关键词: 自适应反步法; 鲁棒控制; 轨迹跟踪; 无人直升机; 干扰估计

中图分类号: TP273　　**文献标识码**: A

Adaptive backstepping-based robust tracking control of unmanned helicopters with disturbances

HE Yue-bang[1], PEI Hai-long[1†], ZHOU Hong-bo[2], SUN Tai-ren[3]

(1. Key Laboratory of Autonomous Systems and Networked Control, Ministry of Education,
South China University of Technology, Guangzhou Guangdong 510640, China;

2. School of Mechanical Engineering, Hunan Institute of Science and Technology, Yueyang Hunan 414006, China;

3. School of Electrical and Information Engineering, Jiangsu University, Zhenjiang Jiangsu 212013, China)

Abstract: This paper presents an adaptive backstepping control method to deal with the problem of robust trajectory tracking for unmanned helicopters with disturbances. The originality of this work relies on the way to compensate the disturbances acting on the helicopter to cause the path deviation. A simplified model is built to facilitate the backstepping controller design; while the unmodelled dynamics is treated as the external wind gusts, mismatched trim values, forces and moments generated by fuselage, fins and other neglected dynamic uncertainties. After designing the backstepping controller, a nonlinear adaptive control law is developed for estimating the disturbance. The estimation results are integrated with the backstepping controller to ensure the robust stability of the closed-loop tracking system. By using the Lyapunov theory, we prove that the designed controller is effective for disturbance rejection, especially for the low frequency disturbances. Two simulations show that the proposed controller outperforms either the conventional backstepping controller or the integral backstepping controller.

Key words: adaptive backstepping; robust control; trajectory tracking; unmanned helicopter; disturbance estimation

1 Introduction

With the capability of hovering, vertical take-off and landing, high levels of agility and maneuverability, unmanned helicopters have significant and remarkable advantages over fixed-wing aircraft in rescue, surveillance, security operation, agricultural and livestock studies, aerial mapping, etc. The helicopter systems, however, are characterized by the highly nonlinear coupling effect between the rotational moments and the translational accelerations and by disturbances like external wind gusts and unavoidably uncertainty due to the empirical representation of aerodynamic forces and moments[1–3]. These disadvantages increase the difficulty in flight control design to improve stability performance and disturbance rejection capability.

Recently the control problems of unmanned helicopters have attracted great attention from control researchers and many control methods have been used to design the flying controller. Based on the identification of the helicopter simplified linear model[4], linear control meth-

Received 28 May 2012; revised 16 August 2012.

†Corresponding author. E-mail: auhlpei@scut.edu.cn; Tel.: +86 13660182029.

This work was supported by the National Natural Science Foundation of China (Nos. 60736024, 61174053), and the Cultivation Fund of the Key Scientific and Technical Innovation Project, Ministry of Education of China (No. 708069).

ods such as traditional PID[5], LQR/LQG[6], H_∞[7], μ-synthesis[8], etc have been used in helicopter's autonomous control successfully. However, these linear control methods can only guarantee the stability and robustness in the neighborhood of the origin. In order to get a large range of stability and robustness, many nonlinear control methods such as gain scheduling[9], MPC[10], adaptive control[11], dynamic inversion[12], feedback linearization[13], neural network[14], backstepping control[15–20], etc are developed. Among these methods, backstepping control aroused many researches' interest in recent years due to the intuitive design process and its guarantee of stability. Robert et al.[15] used backstepping algorithm for helicopter robust trajectory tracking based on a simplified helicopter model. Bilal et al.[16] developed it in a complete model and Adnan et al.[17] added an integral action to the backstepping approach for eliminating the steady state error. Zhou et al.[18] presented a filtering backstopping algorithm for helicopter control in order to reduce the calculation of the virtual control signal derivatives in backstepping design. Lee et al.[19–20] designed an adaptive backstepping integral controller and a backstepping controller with RBFNN for helicopter airdrop missions. However, since the accurate nonlinear model of helicopter could not be obtained due to the empirical representation of aerodynamic forces and moments and external disturbances, the above backstepping algorithms[15–20] would not ensure good tracking performance when the uncertainties and disturbances are considered.

To improve tracking performance and disturbance rejection capability, it is necessary to design a disturbance observer for compensating the disturbances. As the author's investigation, few papers have referred about the disturbance observer design for unmanned helicopters especially for backstepping control design. Francois et al.[21] presented a disturbance observer named extended state observer and used it with approximate feedback linearization control for model-scale helicopters with active wind gusts rejection. Liu et al.[10] designed an explicit nonlinear MPC augmented with disturbance observers which are designed to estimate the influence of the external force/torque introduced by wind turbulences, unmodelled dynamics and variations of the helicopter dynamics. Cheviron[22] used robust differentiation of the measurements to reconstruct the disturbances online accurately and then used robust backstepping techniques for helicopters in presence of wind gusts. This controller provided robust stability but did not compensate for the neglected forces that generated by the main rotor and tail rotor which would result in tracking errors.

In this paper, an adaptive backstepping control is designed for unmanned helicopters with disturbances to do trajectory tracking. For simplifying the helicopter model to fit the adaptive backstepping control design, external wind gusts, mismatched trim values, forces and moments generated by fuselage, fins and other neglected dynamic uncertainties are all treated as lumped disturbances. The adaptive backstepping control is composed of a backstepping control and a nonlinear adaptive control. The backstepping control is used for trajectory tracking, and the nonlinear adaptive control is designed to estimate the lumped disturbances. By integrating the estimated disturbances into backstepping controller, the disturbances can be compensated to reduce the tracking errors. It's shown according to Lyapunov theory that the trajectory tracking errors are robustly stable and the proposed controller is efficient especially for rejecting the low frequency disturbances.

The paper is organized as follows: In Section 2, a helicopter mathematically complete model and its simplified model with disturbances are introduced; Section 3 discusses the design processes of adaptive backstepping used in helicopter controller design and robust stability analysis is carried out to guarantee the feasibility of the proposed controller; Section 4 provides two simulations to demonstrate the performance and merits of the proposed control method; Section 5 concludes the paper.

2 Helicopter modeling

This section is aimed to briefly review the complete nonlinear dynamic model of unmanned helicopters and introduce a simplified nonlinear dynamic model with the other trivial factors that affect dynamics being treated as disturbances. Like the model in [2–3], the unmanned helicopter model is considered as a six-degrees-of-freedom rigid-body model augmented with a simplified rotor dynamic model. For detailed mathematical modeling for full-scale and small-scale helicopters, the reader is referred to [2–3]. Therefore, the complete dynamics of the helicopter can be expressed as

$$\begin{cases} \dot{P} = R(\Theta)V, \\ \dot{V} = -\Omega \times V + \mathrm{g}R(\Theta)^{\mathrm{T}}e_3 + \dfrac{F}{m}, \\ \dot{\Theta} = S(\Theta)\Omega, \\ \dot{\Omega} = -I_{\mathrm{m}}^{-1}\Omega \times I_{\mathrm{m}}\Omega + \Gamma, \end{cases} \tag{1}$$

where g is the acceleration due to a gravity, m is the mass of helicopter, F is the external forces expressed in the body-fixed frame, I_{m} is the diagonal inertia matrix, and Γ is the normalized external torques expressed in the body-fixed frame,

$$e_3 = [0 \ \ 0 \ \ 1]^{\mathrm{T}},\ P = [x \ \ y \ \ z]^{\mathrm{T}}$$

represent the helicopter's inertial position,

$$V = [u \ \ v \ \ w]^{\mathrm{T}}$$

is the velocity expressed in three body axes,

$$\Theta = [\phi \ \ \theta \ \ \psi]^{\mathrm{T}}$$

are attitude angles and

$$\Omega = [p \ \ q \ \ r]^{\mathrm{T}}$$

are angular rates. The rotation matrix R and the attitude kinematic matrix S are defined as

$$R(\Theta) = \begin{bmatrix} c\theta c\psi & s\phi s\theta c\psi - c\phi s\psi & c\phi s\theta c\psi + s\phi s\psi \\ c\theta s\psi & s\phi s\theta s\psi + c\phi c\psi & c\phi s\theta s\psi - s\phi c\psi \\ -s\theta & s\phi c\theta & c\phi c\theta \end{bmatrix}, \tag{2}$$

$$S(\Theta) = \begin{bmatrix} 1 & s\phi t\theta & c\phi t\theta \\ 0 & c\phi & -s\phi \\ 0 & s\phi / c\theta & c\phi / c\theta \end{bmatrix}, \tag{3}$$

where the compact notation $c(\cdot)$, $s(\cdot)$ and $t(\cdot)$ are the shorts for $\cos(\cdot)$, $\sin(\cdot)$ and $\tan(\cdot)$.

The external forces F and moments $\varGamma$ exerting on the helicopter are primarily generated by main and tail rotors thrusts, fins and fuselage drags

$$F=\begin{bmatrix} X_{\rm mr}+X_{\rm fus}\\ Y_{\rm mr}+Y_{\rm fus}+Y_{\rm tr}+Y_{\rm vf}\\ Z_{\rm mr}+Z_{\rm fus}+Z_{\rm ht}\end{bmatrix}, \tag{4}$$

$$\varGamma=\begin{bmatrix} L_{\rm mr}+L_{\rm vf}+L_{\rm tr}\\ M_{\rm mr}+M_{\rm ht}\\ -Q_{\rm e}+N_{\rm tr}+N_{\rm vf}\end{bmatrix}, \tag{5}$$

where the set of forces and moments acting on the helicopter are organized by components: $(\ )_{\rm mr}$ for the main rotor; $(\ )_{\rm tr}$ for the tail rotor; $(\ )_{\rm fus}$ for the fuselage(includes fuselage aerodynamic effects); $(\ )_{\rm vf}$ for the vertical fin and $(\ )_{\rm ht}$ for the horizontal stabilizer, $Q_{\rm e}$ is the torque produced by the engine to counteract the aerodynamic torque on the main rotor blades.

Due to the high complexity and deep couplings of these complete forces (4) and moments (5) which are detailed in [2–3], it is difficult to use them to design controllers directly. This paper only considers the dominating forces and moments which are generated by thrusts of the main and tail rotors and treats others as disturbances, such as

$$F=\begin{bmatrix}0 & 0 & T\end{bmatrix}^{\rm T}+m\begin{bmatrix}d_{\rm u} & d_{\rm v} & d_{\rm w}\end{bmatrix}^{\rm T}, \tag{6}$$

$$\varGamma=\begin{bmatrix} L_{\rm a}a+L_{\rm b}b+d_{\rm p}\\ M_{\rm a}a+M_{\rm b}b+d_{\rm q}\\ N_{\rm r}r+N_{\rm col}\delta_{\rm col}+N_{\rm ped}\delta_{\rm ped}+d_{\rm r}\end{bmatrix}, \tag{7}$$

where T is the main rotor thrust controlled by collective pitch $\delta_{\rm col}$, as

$$T=m(-{\rm g}+Z_{\rm w}w+Z_{\rm col}\delta_{\rm col}),$$

$\delta_{\rm ped}$ is the input of the tail rotor, a and b are flapping angles to depict the flapping of the main rotor along the longitudinal and lateral axis, respectively, $(d_{\rm u},d_{\rm v},d_{\rm w})$ and $(d_{\rm p},d_{\rm q},d_{\rm r})$ are normalized force disturbances and moment disturbances that generated by unmodelled dynamics and external wind gusts. The other parameters can be obtained by system identification in hovering condition. The rotor flapping states a and b cannot be directly measured, but their relationship with lateral and longitudinal cyclic $\delta_{\rm lat}$ and $\delta_{\rm lon}$ can be approximated by the steady state dynamics of the main rotor [10]

$$\begin{cases} a=-\tau q+A_{\rm lat}\delta_{\rm lat}+A_{\rm lon}\delta_{\rm lon},\\ b=-\tau p+B_{\rm lat}\delta_{\rm lat}+B_{\rm lon}\delta_{\rm lon}.\end{cases} \tag{8}$$

Combining (7) and (8), a modified torque input can be expressed as

$$\varGamma=\begin{bmatrix} -\tau(L_{\rm a}q+L_{\rm b}p)\\ -\tau(M_{\rm a}q+M_{\rm b}p)\\ N_{\rm r}r+N_{\rm col}\delta_{\rm col}\end{bmatrix}+\begin{bmatrix} L_{\rm lat}\delta_{\rm lat}+L_{\rm lon}\delta_{\rm lon}+d_{\rm p}\\ M_{\rm lat}\delta_{\rm lat}+M_{\rm lon}\delta_{\rm lon}+d_{\rm q}\\ N_{\rm ped}\delta_{\rm ped}+d_{\rm r}\end{bmatrix}=$$
$$A\varOmega+B\boldsymbol{u}+\begin{bmatrix}d_{\rm p} & d_{\rm q} & d_{\rm r}\end{bmatrix}^{\rm T}, \tag{9}$$

where

$$L_{\rm lat}=L_{\rm a}A_{\rm lat}+L_{\rm b}B_{\rm lat},\ L_{\rm lon}=L_{\rm a}A_{\rm lon}+L_{\rm b}B_{\rm lon},$$
$$M_{\rm lat}=M_{\rm a}A_{\rm lat}+M_{\rm b}B_{\rm lat},$$
$$M_{\rm lon}=M_{\rm a}A_{\rm lon}+M_{\rm b}B_{\rm lon},$$
$$A=\begin{bmatrix} -\tau L_{\rm b} & -\tau L_{\rm a} & 0\\ -\tau M_{\rm b} & -\tau M_{\rm a} & 0\\ 0 & 0 & N_{\rm r}\end{bmatrix},$$
$$B=\begin{bmatrix} 0 & L_{\rm lon} & L_{\rm lat} & 0\\ 0 & M_{\rm lon} & M_{\rm lat} & 0\\ N_{\rm col} & 0 & 0 & N_{\rm ped}\end{bmatrix},$$

$\boldsymbol{u}=\begin{bmatrix}\delta_{\rm col} & \delta_{\rm lon} & \delta_{\rm lat} & \delta_{\rm ped}\end{bmatrix}^{\rm T}$ is the control input.

Note that for avoiding the trimming process in real life operations, the trimming values can be considerd as disturbances that are contained in $(d_{\rm w},d_{\rm p},d_{\rm q},d_{\rm r})$.

Combining (1) (6) and (9), the simplified helicopter model can be expressed in a general affine form

$$\dot{\boldsymbol{x}}=f(\boldsymbol{x})+g_1\boldsymbol{u}+g_2\boldsymbol{d}, \tag{10}$$

where

$$\boldsymbol{x}=[P^{\rm T}\ \ V^{\rm T}\ \ \varTheta^{\rm T}\ \ \varOmega^{\rm T}]^{\rm T}$$

is the helicopter state, and

$$\boldsymbol{d}=\begin{bmatrix}d_{\rm u} & d_{\rm v} & d_{\rm w} & d_{\rm p} & d_{\rm q} & d_{\rm r}\end{bmatrix}^{\rm T}$$

is the lumped disturbance acting on the helicopter,

$$f(\boldsymbol{x})=\begin{bmatrix} R(\varTheta)V\\ -\varOmega\times V+gR(\varTheta)^{\rm T}e_3+(-{\rm g}+Z_{\rm w}w)e_3\\ S(\varTheta)\varOmega\\ -I_{\rm m}^{-1}\varOmega\times I_{\rm m}\varOmega+A\varOmega\end{bmatrix},$$
$$g_1=[\mathbf{0}_{4\times3}\ \ [Z_{\rm col}e_3\ \ \mathbf{0}_{3\times3}]^{\rm T}\ \ \mathbf{0}_{4\times3}\ \ B^{\rm T}]^{\rm T},$$
$$g_2=\begin{bmatrix}\mathbf{0}_{3\times3} & I_3 & \mathbf{0}_{3\times3} & \mathbf{0}_{3\times3}\\ \mathbf{0}_{3\times3} & \mathbf{0}_{3\times3} & \mathbf{0}_{3\times3} & I_3\end{bmatrix}^{\rm T}.$$

Since all the states can be measured and all the parameters in $f(\boldsymbol{x})$, g_1 can be measured or obtained by system identification in hovering condition, the only unknown variable in (10) is the disturbance $\boldsymbol{d}$. In the next section, this paper will design an nonlinear adaptive law to estimate this unknown disturbance $\boldsymbol{d}$ for improving the robust performance and trajectory tracking performance.

3 Adaptive backstepping control with disturbances

In this section an adaptive backstepping control is proposed based on the simplified dynamic model of unmanned helicopter with unmodeled dynamics and external disturbances being treated as a lumped disturbances. The control strategy is to find an adaptive control law for disturbance observing and integrate the estimated disturbances into backstepping control design to improve the trajectory tracking performance. For the purpose of trajectory tracking, the outputs of interest are chosen to be the position vector $P_{\rm r}$ and heading angle $\phi_{\rm r}$. Since the backstepping control is a recursive procedure for systematically selecting the control Lyapunov functions, the position vector $P_{\rm r}$, the heading angle $\phi_{\rm r}$ and the time derivatives $(\dot{P}_{\rm r},\ddot{P}_{\rm r},\dddot{P}_{\rm r},P_{\rm r}^{(4)},\dot{\phi}_{\rm r},\ddot{\phi}_{\rm r})$ are needed for the desired trajectories. The detailed design procedures are presented as the following steps.

Step 1 Define the position tracking error as the item $\delta_1 \in \mathbb{R}^3$ by

$$\delta_1 = P - P_{\rm r}. \tag{11}$$

Using (1) and differentiating (11) yields

$$\dot{\delta}_1 = R(\Theta)V - \dot{P}_{\rm r} + R(\Theta)V_{\rm r} - R(\Theta)V_{\rm r} = -k_1\delta_1 + R(\Theta)\delta_2, \tag{12}$$

where k_1 is the tuning gain with positive value, $V_{\rm r}$ is the desired velocity and is chosen as follows:

$$V_{\rm r} = R(\Theta)^{\rm T}(-k_1\delta_1 + \dot{P}_{\rm r}). \tag{13}$$

Define the Lyapunov function candidate for δ_1 to be

$$V_1 = \frac{1}{2}\delta_1^{\rm T}\delta_1. \tag{14}$$

From (12), the time derivative of V_1 is

$$\dot{V}_1 = -k_1\delta_1^{\rm T}\delta_1 + \delta_1^{\rm T}R(\Theta)\delta_2. \tag{15}$$

Step 2 The velocity tracking error item $\delta_2 \in \mathbb{R}^3$ is chosen in Step 1 as

$$\delta_2 = V - V_{\rm r}. \tag{16}$$

Taking the time derivative of δ_2 and using (1)(6)(12)–(13) yields

$$\dot{\delta}_2 = -\Omega \times V + {\rm g}R(\Theta)^{\rm T}e_3 + \frac{F}{m} - \dot{V}_{\rm r} = -\Omega \times \delta_2 + (-{\rm g} + Z_{\rm w}w + Z_{\rm col}\delta_{\rm col})e_3 + H_1\boldsymbol{d} + R(\Theta)^{\rm T}({\rm g}e_3 - k_1^2\delta_1 - \ddot{P}_{\rm r}) + k_1\delta_2, \tag{17}$$

where $H_1 = [I_3 \;\; \mathbf{0}_{3\times3}]$.

Since the disturbance $\boldsymbol{d}$ is unknown, the estimated disturbance $\hat{\boldsymbol{d}}$ is used to replace $\boldsymbol{d}$ in the following equations. Therefore, (17) can be

$$\dot{\delta}_2 = -\Omega \times \delta_2 + (-{\rm g} + Z_{\rm w}w + Z_{\rm col}\delta_{\rm col})e_3 + H_1\hat{\boldsymbol{d}} + R(\Theta)^{\rm T}({\rm g}e_3 - k_1^2\delta_1 - \ddot{P}_{\rm r}) + k_1\delta_2 + H_1\tilde{\boldsymbol{d}}, \tag{18}$$

where $\tilde{\boldsymbol{d}} = \boldsymbol{d} - \hat{\boldsymbol{d}}$ is the estimation error of the disturbance.

Define a new error

$$\tilde{\delta}_3 = (-{\rm g} + Z_{\rm w}w + Z_{\rm col}\delta_{\rm col})e_3 + H_1\hat{\boldsymbol{d}} + R(\Theta)^{\rm T}M_\delta + \tilde{k}\delta_2, \tag{19}$$

where $M_\delta = {\rm g}e_3 + (1 - k_1^2)\delta_1 - \ddot{P}_{\rm r}$, $\tilde{k} = k_1 + k_2$ and k_2 is the tuning gain with positive value.

Then the time derivative of δ_2 is rewritten as

$$\dot{\delta}_2 = -\Omega \times \delta_2 - k_2\delta_2 - R^{\rm T}(\Theta)\delta_1 + \tilde{\delta}_3 + H_1\tilde{\boldsymbol{d}}. \tag{20}$$

Define the Lyapunov function candidate containing δ_2 by

$$V_2 = V_1 + \frac{1}{2}\delta_2^{\rm T}\delta_2. \tag{21}$$

From (15) and (20), the time derivative of V_2 is represented by

$$\dot{V}_2 = -\delta_2^{\rm T}(\Omega \times \delta_2) - \sum_{i=1}^{2} k_i\delta_i^{\rm T}\delta_i + \delta_2^{\rm T}\tilde{\delta}_3 + \delta_2^{\rm T}H_1\tilde{\boldsymbol{d}}. \tag{22}$$

The cross property makes the first term zero, so

$$\dot{V}_2 = -\sum_{i=1}^{2} k_i\delta_i^{\rm T}\delta_i + \delta_2^{\rm T}\tilde{\delta}_3 + \delta_2^{\rm T}H_1\tilde{\boldsymbol{d}}. \tag{23}$$

At this stage the collective control input $\delta_{\rm col}$ appears in the equation (19). We can choose it to satisfy

$$e_3^{\rm T}\tilde{\delta}_3 = 0. \tag{24}$$

Inserting (19) to (24), the desired collective control $\delta_{\rm col}$ is

$$\delta_{\rm col} = \frac{1}{Z_{\rm col}}({\rm g} - Z_{\rm w}w - e_3^{\rm T}(R(\Theta)^{\rm T}M_\delta + \tilde{k}\delta_2 + H_1\hat{\boldsymbol{d}})). \tag{25}$$

Along the condition of (24), the error $\tilde{\delta}_3$ can be re-expressed as

$$\tilde{\delta}_3 = (E + e_3e_3^{\rm T})\tilde{\delta}_3 = E\tilde{\delta}_3 = E(R(\Theta)^{\rm T}M_\delta + \tilde{k}\delta_2 + H_1\hat{\boldsymbol{d}}), \tag{26}$$

where $E = {\rm diag}\{1, 1, 0\}$.

Step 3 The third error item $\delta_3 \in \mathbb{R}^3$ is defined as

$$\delta_3 = \tilde{\delta}_3 + e_3(\psi - \psi_{\rm r}). \tag{27}$$

By multiplying E in both sides of (27) and using (26), $\tilde{\delta}_3$ can be rewritten as

$$\tilde{\delta}_3 = E\delta_3. \tag{28}$$

Taking the time derivative of δ_3 and recalling (1)(12)(19)–(20)(28) yields

$$\dot{\delta}_3 = \dot{\tilde{\delta}}_3 + e_3(\dot{\psi} - \dot{\psi}_{\rm r}) = E(sk(R(\Theta)^{\rm T}M_\delta)\Omega + R(\Theta)^{\rm T}\dot{M}_\delta + \tilde{k}\dot{\delta}_2) + e_3(e_3^{\rm T}S(\Theta)\Omega - \dot{\psi}_{\rm r}) + EH_1\dot{\hat{\boldsymbol{d}}} = N_1\Omega + N_2 + E\tilde{k}H_1\tilde{\boldsymbol{d}}, \tag{29}$$

where

$$N_1 = Esk(R(\Theta)^{\rm T}M_\delta + \tilde{k}\delta_2) + e_3e_3^{\rm T}S(\Theta),$$
$$N_2 = E(R(\Theta)^{\rm T}((k_1^3 - k_1 - \tilde{k})\delta_1 - \dddot{P}_{\rm r}) + (1 - k_1^2 - \tilde{k}k_2)\delta_2 + \tilde{k}\delta_3 + H_1\dot{\hat{\boldsymbol{d}}}) - e_3\dot{\psi}_{\rm r},$$

and $sk(\cdot)$ denotes the skew-symmetric matrix.

Define a new variable

$$\boldsymbol{\alpha} = \begin{bmatrix}\alpha_1 & \alpha_2 & \alpha_3\end{bmatrix}^{\rm T} = R(\Theta)^{\rm T}((1 - k_1^2)\delta_1 - \ddot{P}_{\rm r}) + \tilde{k}\delta_2, \tag{30}$$

By using the fact $R(\Theta)^{\rm T}R(\Theta) = I$, the following inequality is obtained:

$$\|\boldsymbol{\alpha}\| = \sqrt{\alpha_1^2 + \alpha_2^2 + \alpha_3^2} \leqslant \|(1 - k_1^2)\delta_1\| + \tilde{k}\|\delta_2\| + \|\ddot{P}_{\rm r}\|, \tag{31}$$

where $\|\,.\,\|$ denotes for the Euclidean norm.

With substitution of the definition of M_δ and (30), N_1 can be rewritten as

$$N_1 = Esk(R(\Theta)^{\rm T}ge_3 + \boldsymbol{\alpha}) + e_3e_3^{\rm T}S(\Theta) = \begin{bmatrix} 0 & -gc\phi c\theta - \alpha_3 & {\rm g}s\phi c\theta + \alpha_2 \\ gc\phi c\theta + \alpha_3 & 0 & gs\theta - \alpha_1 \\ 0 & \dfrac{s\phi}{c\theta} & \dfrac{c\phi}{c\theta} \end{bmatrix}, \tag{32}$$

then the determinant of N_1 can be calculated as

$$\det(N_1) = (gc\phi c\theta + \alpha_3)({\rm g} + \frac{\alpha_2 s\phi + \alpha_3 c\phi}{c\theta}). \tag{33}$$

Comparing (33) and (31), a sufficient condition for $\det(N_1) \neq 0$ (N_1 non-singular) is

$$\|(1-k_1^2)\delta_1\| + \tilde{k}\|\delta_2\| + \|\ddot{P}_{\rm r}\| < gc\phi c\theta. \quad (34)$$

Since $\phi, \theta \in (-\frac{\pi}{4}, \frac{\pi}{4})$ for most helicopter flight trajectory, the above inequation is almost true. If the above inequation is not tenable at some time for aggressive flight, one can reduce $\|\ddot{P}_{\rm r}\|$ or $\|\delta_1\|$, $\|\delta_2\|$ by modifying $P_{\rm r}$ and $\dot{P}_{\rm r}$ (see the definition of δ_1, δ_2) to guarantee it tenable. The explication can be thinked that the flight trajectory is too aggressive for the proposed controller to be tracked and must be modified. It is noted that this modification only results in more tracking errors. Thus, we can always assume N_1 is non-singular.

Take

$$\Omega_{\rm r} = -N_1^{-1}(k_3\delta_3 + E\delta_2 + N_2)$$

as a virtual control, then the time derivative of δ_3 is

$$\dot{\delta}_3 = -k_3\delta_3 - E\delta_2 + N_1(\Omega - \Omega_{\rm r}) + E\tilde{k}H_1\tilde{\boldsymbol{d}} = -k_3\delta_3 - E\delta_2 + N_1\delta_4 + E\tilde{k}H_1\tilde{\boldsymbol{d}}, \quad (35)$$

where k_3 is the tuning gain with positive value.

Define the Lyapunov function candidate including δ_3 by

$$V_3 = V_2 + \frac{1}{2}\delta_3^{\rm T}\delta_3 \quad (36)$$

From (23) (28) and (35), the time derivative of V_3 is represented by

$$\dot{V}_3 = -\sum_{i=1}^{3} k_i\delta_i^{\rm T}\delta_i + \delta_3^{\rm T}N_1\delta_4 + (\delta_2^{\rm T} + \delta_3^{\rm T}E\tilde{k})H_1\tilde{\boldsymbol{d}}. \quad (37)$$

Step 4 The angular velocity error item $\delta_4 \in \mathbb{R}^3$ selected in Step 3 is

$$\delta_4 = \Omega - \Omega_{\rm r}. \quad (38)$$

Taking the time derivative of δ_4 and recalling (7) yields

$$\dot{\delta}_4 = \dot{\Omega} - \dot{\Omega}_{\rm r} = H(f(\boldsymbol{x}) + g_1\boldsymbol{u} + g_2\boldsymbol{d}) - \dot{\Omega}_{\rm r}, \quad (39)$$

where $H = [\,\mathbf{0}_{3\times 9} \;\; I_3\,]$.

After sophisticated computations, $\dot{\Omega}_{\rm r}$ can be calculated.

$$\begin{aligned}\dot{\Omega}_{\rm r} = & -N_1^{-1}(k_3(-k_3\delta_3 - E\delta_2 + N_1\delta_4) + \dot{N}_{2-\rm no} + \\ & \dot{N}_{1-\rm no}\Omega_{\rm r} + E(\delta_3 - \Omega\delta_2 - k_2\delta_2 - R(\Theta)^{\rm T}\delta_1) + \\ & E(2 + k_1k_2 + k_3\tilde{k} - sk(\Omega_{\rm r})\tilde{k})H_1\dot{\tilde{\boldsymbol{d}}}),\end{aligned} \quad (40)$$

where

$$\begin{aligned}\dot{N}_{1-\rm no} = & Esk(sk(R(\Theta)^{\rm T}M_\delta + \tilde{k}\delta_2)\Omega + \\ & R(\Theta)^{\rm T}((k_1^3 - k_1 - \tilde{k})\delta_1 - \ddot{P}_{\rm r}) + \\ & (1 - k_1^2 - \tilde{k}k_2)\delta_2 + E\tilde{k}\delta_3) + e_3e_3^{\rm T}\dot{S}(\Theta), \\ \dot{N}_{2-\rm no} = & E(-sk(\Omega)R(\Theta)^{\rm T}((k_1^3 - k_1 - \tilde{k})\delta_1 - \dddot{P}_{\rm r}) + \\ & R(\Theta)^{\rm T}((k_1^3 - k_1 - \tilde{k})(-k_1\delta_1 + R(\Theta)\delta_2) - \\ & P_{\rm r}^{(4)}) + (1 - k_1^2 - \tilde{k}k_2)(-sk(\Omega)\delta_2 - \\ & k_2\delta_2 - R(\Theta)^{\rm T}\delta_1 + E\delta_3) + \\ & \tilde{k}(-k_3\delta_3 - E\delta_2 + N_1\delta_4) + H_1\ddot{\mathbf{d}}) - e_3\ddot{\psi}_{\rm r}.\end{aligned}$$

From (40), one can simplify the description of $\dot{\omega}_{\rm r}$ into two parts with and without estimation errors $\tilde{\boldsymbol{d}}$ as below:

$$\dot{\Omega}_{\rm r} = \dot{\Omega}_{r-\rm no} + N_1^{-1}E(2 + k_1k_2 + k_3\tilde{k} - sk(\Omega_{\rm r})\tilde{k})H_1\dot{\tilde{\boldsymbol{d}}}. \quad (41)$$

Using (41) and assigning $Hg_1\boldsymbol{u}$ as

$$Hg_1\boldsymbol{u} = -H(f(\boldsymbol{x}) + g_2\hat{\boldsymbol{d}}) + \dot{\Omega}_{r-\rm no} - k_4\delta_4 - N_1^{\rm T}\delta_3, \quad (42)$$

then

$$\dot{\delta}_4 = \dot{\Omega} - \dot{\Omega}_{\rm r} = -k_4\delta_4 - N_1^{\rm T}\delta_3 + C(\Omega_{\rm r})\tilde{\boldsymbol{d}}, \quad (43)$$

where k_4 is the tuning gain with positive value,

$$C(\Omega_{\rm r}) = Hg_2 - N_1^{-1}E(2 + k_1k_2 + k_3\tilde{k} - sk(\Omega_{\rm r})\tilde{k})H_1.$$

Let all terms on the right hand side of (25) be expressed by a number s_1 and all terms on the right hand side of (42) be expressed by a vector s_2. Then, combining (25) and (42), one can easily obtain the control law

$$\boldsymbol{u} = \begin{bmatrix} [1 \;\; 0 \;\; 0 \;\; 0] \\ Hg_1 \end{bmatrix}^{-1} \begin{bmatrix} s_1 \\ s_2 \end{bmatrix}. \quad (44)$$

Define the Lyapunov function candidate containing δ_4 by

$$V_4 = V_3 + \frac{1}{2}\delta_4^{\rm T}\delta_4 + \frac{1}{2}\gamma\tilde{\boldsymbol{d}}^{\rm T}\tilde{\boldsymbol{d}}, \quad (45)$$

where γ is a designed positive constant.

From (37) and (43), the time derivative of V_4 can be

$$\begin{aligned}\dot{V}_4 = & -\sum_{i=1}^{4} k_i\delta_i^{\rm T}\delta_i + \tilde{C}(\delta)^{\rm T}\tilde{\boldsymbol{d}} + \gamma\tilde{\boldsymbol{d}}^{\rm T}\dot{\tilde{\boldsymbol{d}}} = \\ & -\sum_{i=1}^{4} k_i\delta_i^{\rm T}\delta_i + \tilde{C}(\delta)^{\rm T}\tilde{\boldsymbol{d}} + \gamma\tilde{\boldsymbol{d}}^{\rm T}(\dot{\boldsymbol{d}} - \dot{\hat{\boldsymbol{d}}}) \leqslant \\ & -\sum_{i=1}^{4} k_i\delta_i^{\rm T}\delta_i + \lambda\dot{\boldsymbol{d}}^{\rm T}\dot{\boldsymbol{d}} - \\ & \gamma\tilde{\boldsymbol{d}}^{\rm T}(\dot{\hat{\boldsymbol{d}}} - \gamma^{-1}\tilde{C}(\delta) - \frac{\gamma}{4\lambda}\tilde{\boldsymbol{d}}),\end{aligned} \quad (46)$$

where

$$\delta = \begin{bmatrix} \delta_1^{\rm T} & \delta_2^{\rm T} & \delta_3^{\rm T} & \delta_4^{\rm T} \end{bmatrix}^{\rm T},$$
$$\tilde{C}(\delta) = H_1^{\rm T}(\delta_2 + E\tilde{k}\delta_3) + C(\Omega_{\rm r})^{\rm T}\delta_4,$$

λ is a designed positive constant.

The last term in (46) can be eliminated by updating the estimated disturbances in the following way

$$\dot{\hat{\boldsymbol{d}}} = \gamma^{-1}\tilde{C}(\delta) + \frac{\gamma}{4\lambda}\tilde{\boldsymbol{d}}. \quad (47)$$

Since $\tilde{\boldsymbol{d}}$ can be rewritten as

$$\tilde{\boldsymbol{d}} = \boldsymbol{d} - \hat{\boldsymbol{d}} = g_2^{+}(\dot{\boldsymbol{x}} - f(\boldsymbol{x}) - g_1\boldsymbol{u}) - \hat{\boldsymbol{d}}, \quad (48)$$

where $g_2^{+} = (g_2^{\rm T}g_2)^{-1}g_2^{\rm T}$. The updating law of the estimated disturbance $\hat{\boldsymbol{d}}$ in (47) can be reachieved as

$$\begin{cases} \hat{\boldsymbol{d}} = \boldsymbol{d}_{\mathbf{c}} + \dfrac{\gamma}{4\lambda}g_2^{+}\boldsymbol{x}, \\ \dot{\boldsymbol{d}}_{\mathbf{c}} = \gamma^{-1}\tilde{C}(\delta) - \dfrac{\gamma}{4\lambda}(\hat{\boldsymbol{d}} + g_2^{+}(f(\boldsymbol{x}) + g_1\boldsymbol{u})). \end{cases} \quad (49)$$

Inserting (47) to (46) results in

$$\dot{V}_4 \leqslant -\sum_{i=1}^{4} k_i\delta_i^{\rm T}\delta_i + \lambda\dot{\boldsymbol{d}}^{\rm T}\dot{\boldsymbol{d}}, \quad (50)$$

then V_4 decreases when

$$\sum_{i=1}^{4} k_i \delta_i^{\mathrm{T}} \delta_i > \lambda \dot{\boldsymbol{d}}^{\mathrm{T}} \dot{\boldsymbol{d}},$$

which indicates that the tracking errors are uniformly ultimately bounded by

$$\sum_{i=1}^{4} k_i \delta_i^{\mathrm{T}} \delta_i \leqslant \lambda \dot{\boldsymbol{d}}^{\mathrm{T}} \dot{\boldsymbol{d}}$$

if $\dot{\boldsymbol{d}}$ is considered as external disturbance and bounded.

Since the model used for control design is a simplified model mentioned in Section 2, $\dot{\boldsymbol{d}}$ may contain the information of states. We should analyze the robust stability of the closed system. Let us define

$$z = \mathrm{diag}\{\sqrt{k_1}, \sqrt{k_2}, \sqrt{k_3}, \sqrt{k_4}\}\delta$$

and only consider the disturbance $\dot{\boldsymbol{d}}$ as model uncertainty which can be expressed as

$$\dot{\boldsymbol{d}} = \Delta z, \tag{51}$$

where Δ denotes the uncertain matrix.

Substituting (51) to (50) yields

$$\dot{V}_4 \leqslant -z^{\mathrm{T}}(I_{12} - \lambda \Delta^{\mathrm{T}} \Delta) z. \tag{52}$$

If uncertain matrix Δ satisfies

$$\Delta^{\mathrm{T}} \Delta < \lambda^{-1} I_{12}, \tag{53}$$

then $\dot{V}_4 < 0$ when $z \neq 0$, which indicates that the closed-loop system is robustly stable. It can be seen from (53) that the robust performance of the closed-loop system can be improved by selecting a sufficiently small λ.

Note that the robust control problem of (51) is a standard H_∞ control problem[23]. By using small-gain theorem[23], the closed-loop system is robustly stable if

$$\sup_{\Delta} \| \Delta \frac{z(s)}{\dot{\boldsymbol{d}}(s)} \|_\infty < 1. \tag{54}$$

From (53) and (54), we have

$$\max_{\omega} \bar{\sigma}(\frac{1}{\mathrm{j}\omega} T_{\mathrm{zd}}(\mathrm{j}\omega)) = \| \frac{1}{s} T_{\mathrm{zd}}(s) \|_\infty = \| \frac{z(s)}{\dot{\boldsymbol{d}}(s)} \|_\infty \leqslant \sqrt{\lambda}, \tag{55}$$

where $\bar{\sigma}(\cdot)$ denotes the maximal singular value, and

$$T_{\mathrm{zd}}(s) = \frac{z(s)}{\boldsymbol{d}(s)}$$

denotes the transfer function from $\boldsymbol{d}$ to z.

From (55), we also have

$$\bar{\sigma}(T_{\mathrm{zd}}(\mathrm{j}\omega)) = |\omega| \bar{\sigma}(\frac{1}{\mathrm{j}\omega} T_{\mathrm{zd}}(\mathrm{j}\omega)) \leqslant |\omega| \max_{\omega} \bar{\sigma}(\frac{1}{\mathrm{j}\omega} T_{\mathrm{zd}}(\mathrm{j}\omega)) \leqslant \sqrt{\lambda} |\omega|, \tag{56}$$

which implies the transfer function $T_{\mathrm{zd}}(s)$ has a zero in the origin. So, under the adaptive backstepping controller, the closed-loop system has zero steady-state error. λ can be considered as a specification of rejecting disturbances which means that smaller λ, better disturbance attenuation. Thus, the presented adaptive backstepping controller is capable of achieving the robust trajectory tracking and disturbance attenuation, especially low frequency rejection. The following theorem summarizes the above-mentioned result.

Theorem 1 Consider the unmanned helicopter with the system model described by (10). If the helicopter's adaptive backstepping control law is designed as (44) with the disturbance estimation updating law (49), then the closed-loop tracking system is robustly stable and the trajectory tracking error is uniformly ultimately bounded if the time derivative of the external disturbances is bounded.

4 Simulation

In this section, two numerical simulations are presented to investigate the performance of the proposed adaptive backstepping controller. The first simulation considers the stabilization in hovering flight with initial position errors, heading angle error and input errors. The second simulation aims at dealing with robust trajectory tracking problem for unmanned helicopter. The two numerical simulations were conducted in the MATLAB environment, where the time steps were set by 0.01s for realizing the controller and simulating the helicopter dynamic model. The controller parameters should be selected to achieve the desired performance defined in ADS-33D-PRF [7] in practical application and this simulation selects them as same as [18] (Table 1). The simplified helicopter's parameters are shown in Table 2. The first and second derivatives of the estimated disturbances $\hat{\boldsymbol{d}}$ are approximately computed by a low pass filter, i.e.

$$\dot{\hat{\boldsymbol{d}}} \approx \dot{\bar{\boldsymbol{d}}} = \omega_{\mathrm{s}}(\hat{\boldsymbol{d}} - \bar{\boldsymbol{d}})$$

for simplifying calculations and filtering the disturbance with high frequency, and the parameter ω_{s} chosen to be 10 is appropriate for unmanned helicopter. The time derivative of the reference trajectory with respect to time and their higher derivatives are dealt with in an ad hoc way by numerical differentiation, i.e.

$$\dot{P}_{\mathrm{r}}(n) \approx \frac{P_{\mathrm{r}}(n) - P_{\mathrm{r}}(n-1)}{\Delta T},$$

where $\Delta T = 0.01\,\mathrm{s}$ is the sample time.

Table 1 Parameters of the proposed controller

Symbol	Description	Value
k_1	The tuning gain for the desired velocity control	0.5
k_2	The tuning gain for the desired error $\tilde{\delta}_3$	1
k_3	The tuning gain for the desired angular rate control	2
k_4	The tuning gain for the desired input	5
$\{\gamma, \lambda\}$	The adaptation gains for the updating rule of disturbance estimation	$\{10, 0.5\}$

Table 2 Parameters of the unmanned helicopter

Symbol	Description	Value
$m/\,\mathrm{kg}$	The mass of helicopter	8.2
$I_{\mathrm{m}}/\,(\mathrm{kg}\cdot\mathrm{m}^2)$	The moment of inertia	$\mathrm{diag}\{0.18, 0.34, 0.28\}$
$\mathrm{g}/\,(\mathrm{m}\cdot\mathrm{s}^{-2})$	The acceleration of gravity	9.8
$Z_{\mathrm{w}}/\,\mathrm{s}^{-1}$	Linkage gain ratio of T to w	-0.7615
$Z_{\mathrm{col}}/\,(\mathrm{m}/(\mathrm{rad}\cdot\mathrm{s}^2))$	Linkage gain ratio of T to δ_{col}	-131.4125
$A/\,\mathrm{s}^{-1}$	Coefficient matrix of Ω in (9)	$\mathrm{diag}\{-48.1757, -25.5048, -0.9808\}$
$B/\,\mathrm{s}^{-2}$	Coefficient matrix of $\boldsymbol{u}$ in (9)	$\begin{bmatrix} 0 & 1.6895 & 0 \\ 0.8945 & 0 & 0 \\ 0 & 0 & 0.1358 \end{bmatrix} \times 10^3$

In order to demonstrate the merits of the proposed adaptive backstepping controller, two controllers using the normal backstepping design and integral backstepping design are also used in these simulation cases for comparison. The normal backstepping controller has the same controller parameters as the proposed controller and the integral backstepping controller adds an integral tuning gains $k_{\mathrm{I}} = 0.5$ and others are also chosen as the same as the proposed controller.

4.1 Hovering simulation

The hovering simulation considers the initial position offset $\delta_1 = [-1\ \ -1\ \ 1]^{\mathrm{T}}\,\mathrm{m}$, heading angle offset $\delta_\psi = -90^\circ$ and inputs mismatched offset

$$\delta_{\mathrm{u}} = [0.01\ \ -0.02\ \ -0.01\ \ -0.025]^{\mathrm{T}}\,\mathrm{rad}.$$

The aim of hovering simulation is to stabilize the unmanned helicopter to the trimmed position $P = [0\ \ 0\ \ 0]^{\mathrm{T}}\,\mathrm{m}$ and heading angle $\psi = 0^\circ$.

Figures 1–4 illustrate the results of the first simulation. It can be seen that the normal backstepping approach is able to deal with the stabilization, but it cannot compensate for the steady-state error. In contrast, the backstepping with integral action cancels the steady state error, but it has side-effects like overshoot. Obviously, the proposed adaptive backstepping control approach outperforms the other two control strategies to a large extent.

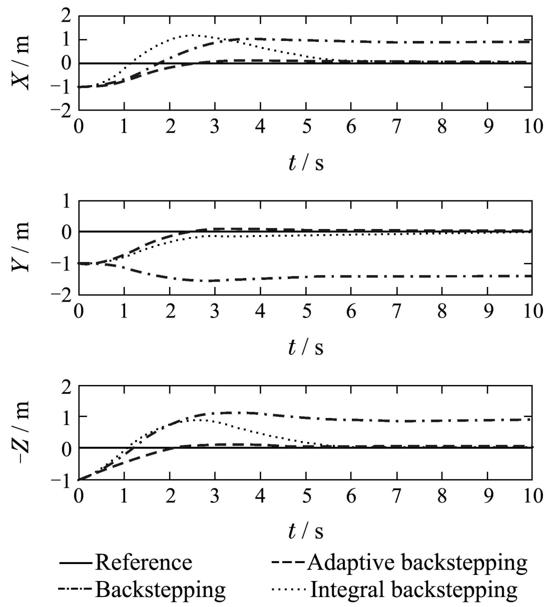

Fig. 1 Position results in hovering

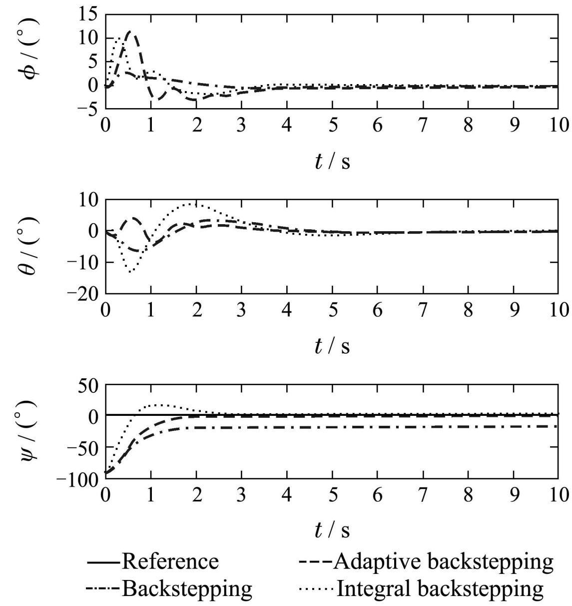

Fig. 2 Attitude angle results in hovering

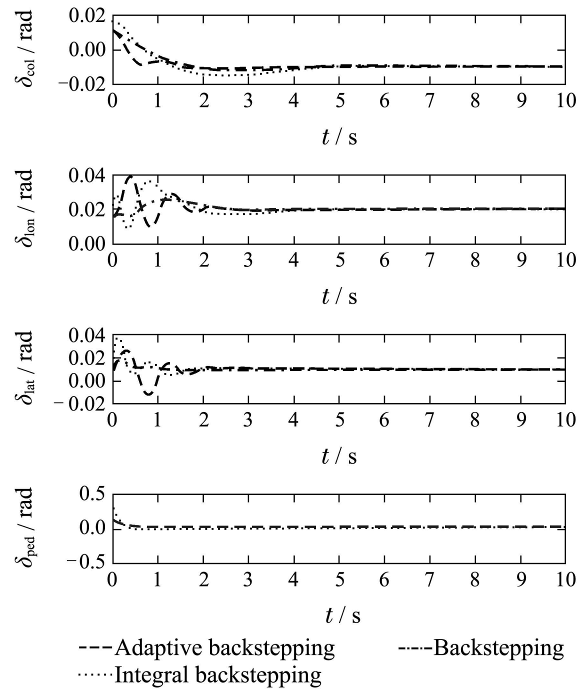

Fig. 3 Control inputs in hovering

Figure 4 shows that the disturbance estimation updating law (49) is efficient for mismatched trimming offsets.

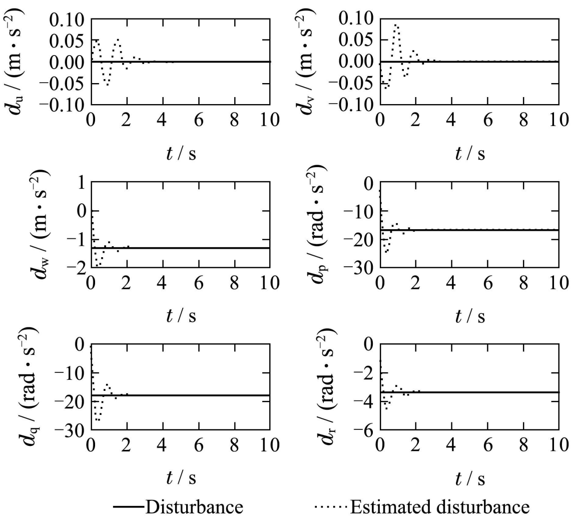

Fig. 4 Estimated disturbances in hovering

4.2 Trajectory tracking with disturbances

In this tracking case, a fast-moving trajectory is designed to be followed, and its position vector is given by

$$P_{\rm r} = [X_{\rm r}\ \ Y_{\rm r}\ \ 0]^{\rm T},$$

and heading angle $\psi_{\rm r} = 0°$, where

$$X_{\rm r} = \begin{cases} t^2, & t \leqslant 5\,{\rm s}, \\ 25 + 10(t-5), & 5\,{\rm s} < t \leqslant 7\,{\rm s}, \\ 45 + (17-t)(t-7), & 7\,{\rm s} < t \leqslant 12\,{\rm s}, \\ 70, & t > 12\,s, \end{cases}$$

$$Y_{\rm r} = \begin{cases} (t-12)^2, & 12\,{\rm s} < t \leqslant 17\,{\rm s}, \\ 25 + 10(t-17), & 17\,{\rm s} < t \leqslant 19\,{\rm s}, \\ 45 + (29-t)(t-19), & 19\,{\rm s} < t \leqslant 24\,{\rm s}, \\ 70, & t > 24\,{\rm s}. \end{cases}$$

In order to verify the robustness of the proposed controller against the model uncertainties and the external disturbances, a disturbance

$$\boldsymbol{d} = \varDelta[V^{\rm T}\ \ \varTheta^{\rm T}\ \ \varOmega^{\rm T}]^{\rm T} + \boldsymbol{d}_{\rm wind}$$

is added in this simulation, where

$$\varDelta \in \mathbb{R}^{6\times 9}$$

represents the model uncertainty and all of its elements are pseudorandom values on the open interval $(-0.5, 0.5)$,

$$\boldsymbol{d}_{\rm wind} = [\frac{\sqrt{2}}{2}v_{\rm wind}\ \ \frac{\sqrt{2}}{2}v_{\rm wind}\ \ \boldsymbol{0}_{1\times 4}]^{\rm T}$$

represents the external disturbance such as wind gust and $v_{\rm wind}$ is governed by a random distribution with a zero mean and processed through a low pass filter which is detailed in [24]. The maximal gain of $v_{\rm wind}$ is designed to be near 2.

The simulation results are shown in Figs.5–9. Fig.5 depicts the results of position tracking affected by the disturbance $\boldsymbol{d}$. Fig. 6 shows its position tracking errors.

Obviously, from Figs.5–6, we can find that the precise trajectory tracking can be achieved by using the proposed control approach.

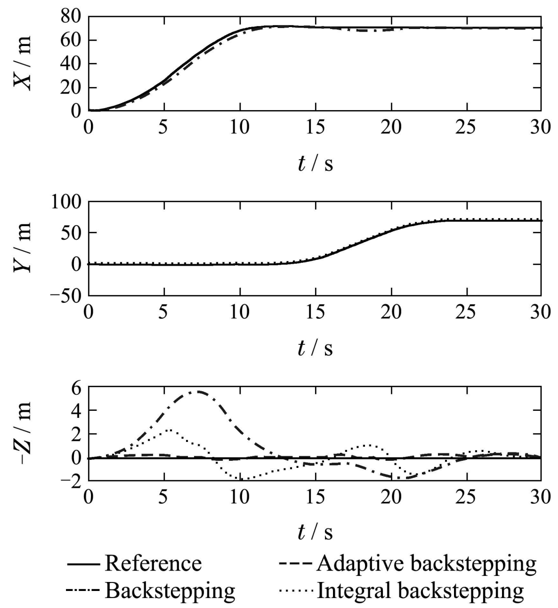

Fig. 5 Position trajectory

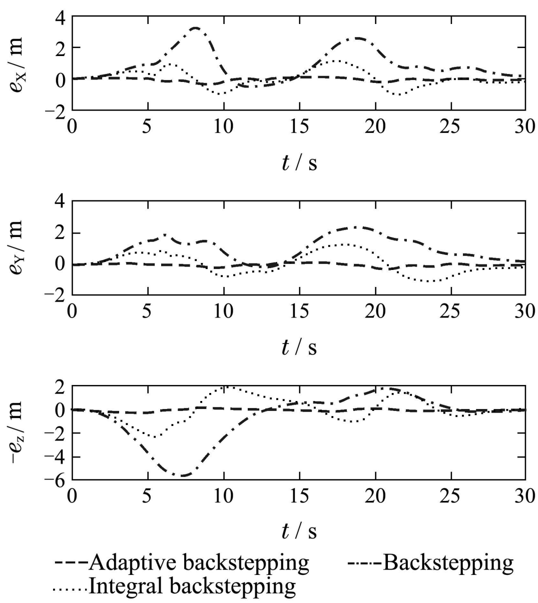

Fig. 6 Position tracking errors

Moreover, From Figs.5–6 and their corresponding obvious tracking errors under the normal backstepping control and integral backstepping scheme, it can be found that the tracking error performance under the proposed control approach is substantially improved, which implies that the proposed control approach is efficient for robust trajectory tracking control of unmanned helicopters with disturbances.

The heading angle tracking results in Fig.7 also illustrates its more excellent tracking performance than the other two methods. From the large variation range of the time responses of roll angle ϕ and pitch angle θ in Fig.7, it indicates that the tracking trajectory is very aggressive. Fig.8 shows the control inputs and Fig.9 illustrates the effectiveness of the designed disturbance estimation updating law (49).

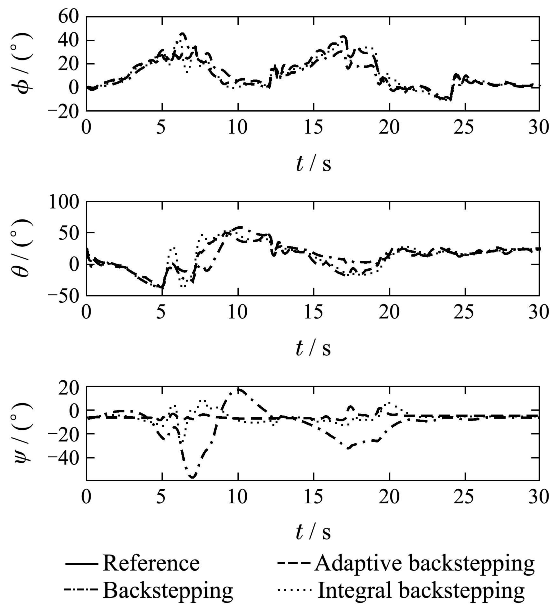

Fig. 7 Attitude angles

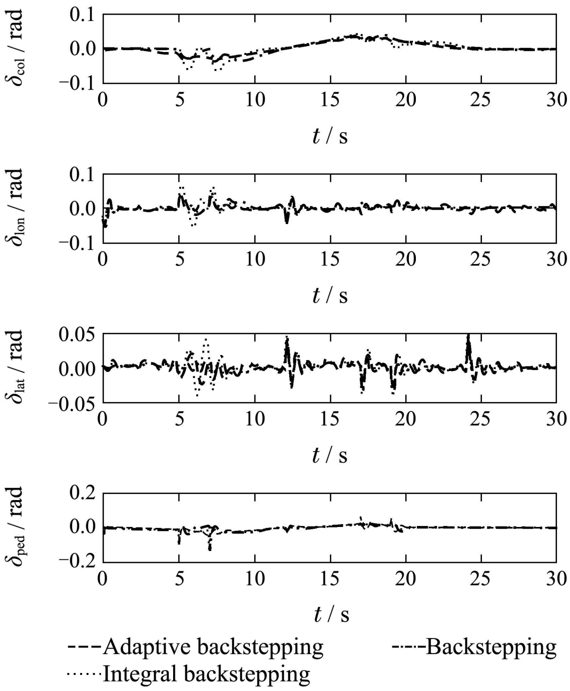

Fig. 8 Control inputs

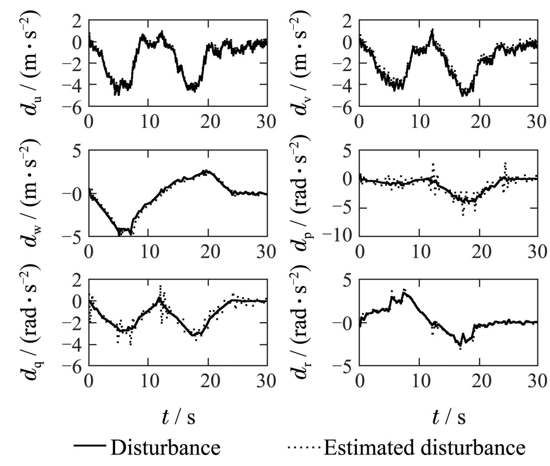

Fig. 9 Estimated disturbances

5 Conclusions

This paper addresses the robust trajectory tracking problem for unmanned helicopters with disturbances. First, a simplified model is established for fitting the backstepping controller design easily with treating the unmodelled dynamics as lumped disturbances which contain external wind gusts, mismatched trim values, the forces and moments generated by fuselage, fins and other neglected dynamic uncertainties. Then a adaptive backstepping controller is designed to ensure desired trajectory tracking, which is a combination of backstepping technique, adaptive control technique. It is shown according to Lyapunov theory that the trajectory tracking errors are robustly stable and the proposed controller is efficient especially for rejecting the low frequency disturbances. Finally, two simulations are used to show that the tracking performance of the closed-loop system used by adaptive ackstepping is more outstanding than used by normal backstepping or integral backstepping.

References:

[1] PADFIELD G D. *Helicopter Flight Dynamics: the Theory and Application of Flying Qualities and Simulation Modeling* [M]. Washington: Blackwell, 2007.

[2] GAVRILETS V. *Autonomous aerobatic maneuvering of miniature helicopters* [D]. Boston: Massachusetts Institute of Technology, 2003.

[3] CAI G, CHEN B M, LEE T H. *Unmanned Rotorcraft Systems* [M]. Heidelberg: Springer, 2011.

[4] METTLER B F. *Identification Modeling and Characteristics of Miniature Rotorcraft* [M]. London: Kluwer Academic Publisher, 2003.

[5] KIM H J, SHIM D H. A flight control system for aerial robots: Algorithms and experiments [J]. *Control Engineering Practice*, 2003, 11(2): 1389 – 1400.

[6] GRIBBLE J J. Linear quadratic Gaussian/loop transfer recovery design for a helicopter in low-speed flight [J]. *Journal of Guidance, Control, and Dynamics*, 1993, 16(4): 754 – 761.

[7] CAI G, CHEN B M, DONG X, et al. Design and implementation of a robust and nonlinear flight control system for an unmanned helicopter [J]. *Mechatronics*, 2011, 21(5): 803 – 820.

[8] MACLAY D, WILLIAMS S J. The use of mu-synthesis in full envelope, helicopter flight control system design [C] //*International Conference on CONTROL '91*. Edinburgh: IEEE, 1991: 718 – 723.

[9] OOSTEROM M, BABUSKA R. Design of a gain-scheduling mechanism for flight control laws by fuzzy clustering [J]. *Control Engineering Practice*, 2006, 14(7): 769 – 781.

[10] LIU C, CHEN W H, JOHN A. Tracking control of small-scale helicopters using explicit nonlinear MPC augmented with disturbance observers [J]. *Control Engineering Practice*, 2012, 20(3): 258 – 268.

[11] REINER J, BALAS G J. Robust dynamic inversion for control of highly maneuverable aircraft [J]. *AIAA Journal of Guidance, Control, and Dynamics*, 1995, 18(1): 18 – 24.

[12] JOHNSON E, KANNAL S. Adaptive trajectory control for autonomous helicopters [J]. *Journal of Guidance, Control and Dynamics*, 2005, 28(3): 524 – 538.

[13] SONG B, LIU Y, FAN C. Feedback linearization of the nonlinear model of a small-scale helicopter [J]. *Journal of Control Theory and Applications*, 2010, 8(3): 301 – 308.

[14] CHEN M, GE S S, REN B. Robust attitude control of helicopters with actuator dynamics using neural networks [J]. *IET Control Theory and Applications*, 2010, 4(12): 2837 – 2854.

[15] ROBERT M, TAREK H. Robust trajectory tracking for a scale model autonomous helicopter [J]. *International Journal of Robust and Nonlinear Control*, 2004, 14(12): 1035 – 1059.

[16] BILAL A, HEMANSHU R P, MATT G. Flight control of a rotary wing UAV using backstepping [J]. *International Journal of Robust and Nonlinear Control*, 2010, 20(6): 639 – 658.

[17] LEE C, TSAI C. Improvement in trajectory tracking control of a small scale helicopter via backstepping [C] //*Proceedings of International Conference on Mecharonics*. Kumamoto: IEEE, 2007: 1 – 6.

[18] ZHOU Hongbo, PEI Hailong, HE Yuebang, et al. Trajectory-tracking control for small unmanned helicopter with state constraints [J]. *Journal of Control Theory and Applications*, 2012, 29(6): 778 – 784. (周洪波, 裴海龙, 贺跃帮, 等. 状态受限的小型无人直升机轨迹跟踪控制 [J]. 控制理论与应用, 2012, 29(6): 778 – 784.)

[19] LEE C, TSAI C. Adaptive backstepping integral control of a small-scale helicopter for airdrop missions [J]. *Asian Journal of Control*, 2010, 12(4): 531 – 541.

[20] LEE C, TSAI C. Improved nonlinear trajectory tracking using RBFNN for a robotic helicopter [J]. *International Journal of Robust an Nonlinear Control*, 2010, 20(10): 1079 – 1096.

[21] FRANCOIS L, ADNAN M, GABRIEL A. Robust nonlinear controls of model-scale helicopters under lateral and vertical wind gusts [J]. *IEEE Transactions on Control Systems Technology*, 2012, 20(1): 154 – 163.

[22] CHEVIRON T. Robust control of an autonomous reduced scale helicopter in presence of wind gusts [C] //*AIAA Guidance, Navigation, and Control Conference and Exhibit*. Keystone: AIAA, 2006: 4545 – 4566.

[23] DOYLE J C, FRANCIS B A, TANNENBAUM A R. *Feedback Control Theory* [M]. New York: MacMillan, 1992.

[24] GADEWADIKAR J, LEWIS F L, SUBBARAO K, et al. H-infinity static output-feedback control for rotorcraft [J]. *Journal of Intelligent and Robotic Systems*, 2009, 54(4): 629 – 646.

作者简介:

贺跃帮 (1983–), 男, 博士研究生, 目前研究方向为无人直升机的辨识与鲁棒非线性控制, E-mail: heyuebag@gmail.com;

裴海龙 (1965–), 男, 教授, 博士生导师, 目前研究方向为非线性控制及人工神经网络, E-mail: auhlpei@scut.edu.cn;

周洪波 (1981–), 男, 博士研究生, 目前研究方向为无人直升机建模及非线性控制, E-mail: zhouhbo@gmail.com;

孙太任 (1985–), 男, 博士研究生, 目前研究方向为非线性系统和神经网络控制, E-mail: suntren@gmail.com